Pairing Fluctuation Effects on the Single-Particle Spectra for the Superconducting State

P. Pieri, L. Pisani, and G. C. Strinati
Dipartimento di Fisica, UdR INFM, Università di Camerino, I-62032 Camerino, Italy
(Received 18 November 2003; published 15 March 2004)

Single-particle spectra are calculated in the superconducting state for a fermionic system with an attractive interaction, as functions of temperature and coupling strength from weak to strong. The fermionic system is described by a single-particle self-energy that includes pairing-fluctuation effects in the superconducting state. The theory reduces to the ordinary BCS approximation in weak coupling and to the Bogoliubov approximation for the composite bosons in strong coupling. Several features of the single-particle spectral function are shown to compare favorably with experimental data for cuprate superconductors.

DOI: 10.1103/PhysRevLett.92.110401 PACS numbers: 03.75.Ss, 03.75.Hh, 05.30.Jp, 74.72.–h

Information on the single-particle spectral function that is obtained from angle-resolved photoemission spectroscopy [1] and tunneling data [2] for cuprate superconductors can shed light on the characteristic features of the superconducting state as well as on its connection with the unconventional normal state above the critical temperature T_c.

Most prominent among these features are the continuous evolution of a broad pseudogap structure from above to below T_c [1,2], the emergence of a coherent peak below T_c that combines with the pseudogap structure to yield a characteristic peak-dip-hump profile [1] (for which two distinct energy scales can be identified), and the peculiar dependence of the frequency position and weight of the coherent peak on temperature and doping [1]. Generally speaking, features of the standard BCS theory are recovered for overdoped samples, while non-BCS behaviors occur for optimally doped and underdoped samples.

The origin of the peak-dip-hump profile has especially been the subject of controversy, being attributed either to "extrinsic" effects such as the bilayer splitting [3] or to "intrinsic"effects. The latter can be identified over and above the extrinsic effects and are believed to originate from strong (many-body) interactions in the system [4].

Quite independently from the microscopic origin of the fermionic attraction giving rise to superconductivity, its strength is believed to be stronger in optimally doped and underdoped than in overdoped samples [5], consistently with the above findings. This implies that pairing fluctuations should definitely be taken into account, irrespective of other effects (such as the bilayer splitting and/or additional many-body effects associated with specific pairing mechanisms [6]).

In this Letter, we assess the role of pairing fluctuations for the single-particle spectral function in the superconducting state on rather general grounds, by identifying a single-particle self-energy that describes fluctuating Cooper pairs in weak coupling and noncondensed composite bosons in strong coupling. (The latter form as bound-fermion pairs in the strong-coupling limit of the fermionic attraction.) To this end, we consider fermions mutually interacting via an attractive contact potential in a 3D continuum, without taking into account lattice effects or the explicit physical mechanism responsible for the attraction. Qualitative comparison with experimental data will thus rest on identifying the increasing coupling strength in this model with the increasing potential strength for a decreasing doping level in the phase diagram of cuprate superconductors. Although the effective model considered here is oversimplified for a full description of cuprates, the physical questions we are addressing are sufficiently general that this minimal model will prove sufficient to capture the main experimental features.

Our main results for the single-particle spectral function (to be compared with the experimental findings) are summarized as follows:

(i) A broad pseudogap structure and a coherent peak are simultaneously present in a wide range of coupling and temperature below T_c, giving rise to a peak-dip-hump profile. Two distinct energy scales (the positions $\Delta_{\rm pg}$ of the broad pseudogap structure and $\Delta_{\rm m}$ of the coherent peak) can then be extracted from the spectra at a given temperature and coupling, as seen experimentally [1].

(ii) At a given (notably, intermediate) coupling, BCS-like features coexist with non-BCS behaviors. The position $\Delta_{\rm m}$ and weight z of the coherent peak versus wave vector follow a BCS-like dependence, as found experimentally [7,8]. At the same time, the weight z of the coherent peak has a strong temperature dependence, in agreement with experiments [9,10] but in contrast with BCS theory.

(iii) At low temperature, the weight z of the coherent peak has a strong dependence on coupling, decreasing monotonically from weak to strong coupling (as seen experimentally in cuprates for decreasing doping [9,10]). At the same time, the position $\Delta_{\rm m}$ of the coherent peak increases monotonically with coupling [9,10].

(iv) The positions $\Delta_{\rm pg}$ of the broad pseudogap structure at T_c and $\Delta_{\rm m}$ of the coherent peak near zero temperature cross each other as a function of coupling about

 0031-9007/04/92(11)/110401(4)$22.50

intermediate coupling. This feature is also seen experimentally by intrinsic tunneling experiments at different dopings [11] (although these data are subject to controversy [12]).

Pairing fluctuations are taken into account in our theory by considering, besides the off-diagonal BCS-like self-energy, the diagonal t-matrix self-energy suitably extended to the superconducting state (we use the Nambu formalism throughout). The t-matrix self-energy has been widely used to include pairing fluctuations in the normal state [13] and, specifically, to account for pseudogap features in the single-particle spectral function [14]. In our theory, the diagonal t-matrix self-energy (that survives above T_c) will essentially be responsible for the presence of the broad pseudogap structure below T_c. The off-diagonal BCS-like self-energy will instead give rise to the simultaneous emergence of the coherent peak. In addition, our theory recovers the Bogoliubov approximation for the composite bosons in strong coupling [15].

The diagonal t-matrix self-energy reads

$$\Sigma_{11}(k) = -\int \frac{d\mathbf{q}}{(2\pi)^3} \frac{1}{\beta} \sum_{\Omega_\nu} \Gamma_{11}(q) \mathcal{G}_{11}(q-k), \quad (1)$$

while the off-diagonal self-energy has the BCS-like form $\Sigma_{12}(k) = -\Delta$ in terms of the superconducting order parameter Δ. The pairing-fluctuation propagator Γ_{11} in the broken-symmetry phase entering Eq. (1) is given by

$$\Gamma_{11}(q) = \frac{\chi_{11}(-q)}{\chi_{11}(q)\chi_{11}(-q) - \chi_{12}(q)^2}, \quad (2)$$

with

$$-\chi_{11}(q) = \frac{m}{4\pi a_F} + \int \frac{d\mathbf{p}}{(2\pi)^3} \left[\frac{1}{\beta} \sum_{\omega_n} \mathcal{G}_{11}(p+q)\mathcal{G}_{11}(-p) - \frac{m}{\mathbf{p}^2} \right], \quad (3)$$

$$\chi_{12}(q) = \int \frac{d\mathbf{p}}{(2\pi)^3} \frac{1}{\beta} \sum_{\omega_n} \mathcal{G}_{12}(p+q)\mathcal{G}_{21}(-p). \quad (4)$$

In the above expressions, $q = (\mathbf{q}, \Omega_\nu)$, $k = (\mathbf{k}, \omega_l)$, and $p = (\mathbf{p}, \omega_n)$ ($\mathbf{q}$, $\mathbf{k}$, and $\mathbf{p}$ being wave vectors, Ω_ν a bosonic Matsubara frequency, and ω_l and ω_n fermionic Matsubara frequencies), m is the fermionic mass, β is the inverse temperature, and $\mathcal{G}_{ij}$ $(i, j = 1, 2)$ have the form of the BCS single-particle Green's functions in Nambu notation.

For a given temperature and strength of the point-contact interaction, the chemical potential μ and the order parameter Δ are obtained by solving the coupled particle number and gap equations:

$$n = 2\int \frac{d\mathbf{k}}{(2\pi)^3} \frac{1}{\beta} \sum_{\omega_l} e^{i\omega_l \eta} G_{11}(\mathbf{k}, \omega_l), \quad (5)$$

$$-\frac{m}{4\pi a_F} = \int \frac{d\mathbf{k}}{(2\pi)^3} \left\{ \frac{\tanh[\beta E(\mathbf{k})/2]}{2E(\mathbf{k})} - \frac{m}{\mathbf{k}^2} \right\}, \quad (6)$$

where $\eta = 0^+$ and $E(\mathbf{k}) = [\xi(\mathbf{k})^2 + \Delta^2]^{1/2}$ with $\xi(\mathbf{k}) = \mathbf{k}^2/(2m) - \mu$. The scattering length a_F of the (fermionic) two-body problem has been introduced to eliminate the ultraviolet divergences originating from the use of a point-contact interaction. The dimensionless parameter $(k_F a_F)^{-1}$ [where k_F is the Fermi wave vector related to the density n via $k_F = (3\pi^2 n)^{1/3}$] characterizes the fermionic coupling strength and ranges formally from $-\infty$ to $+\infty$. [Correspondingly, the Fermi energy ε_F equals $k_F^2/(2m)$.] In practice, the crossover from the weak- to strong-coupling regimes occurs in the limited range $-1 \lesssim (k_F a_F)^{-1} \lesssim +1$, which will be mostly explored in what follows. The dressed normal (diagonal) Green's function G_{11} in Eq. (5) is obtained by matrix inversion of the Dyson's equation in Nambu formalism with the above self-energies and is given by:

$$G_{11}(\mathbf{k}, \omega_l) = \left[i\omega_l - \xi(\mathbf{k}) - \Sigma_{11}(\mathbf{k}, \omega_l) - \frac{\Delta^2}{i\omega_l + \xi(\mathbf{k}) + \Sigma_{11}(\mathbf{k}, -\omega_l)} \right]^{-1}. \quad (7)$$

Note that, while Eq. (5) contains the dressed normal (diagonal) Green's function, the gap Eq. (6) is obtained from the anomalous (off-diagonal) BCS Green's function and thus its form is not modified with respect to the BCS theory. This ensures that the pairing-fluctuation propagator (2) remains gapless for all temperatures (below T_c) and couplings and that the Bogoliubov approximation is recovered for the composite bosons — see below. [The value of T_c is obtained from Eqs. (5) and (6) by setting $\Delta = 0$ identically.] The numerical values of the chemical potential μ and order parameter Δ at a given temperature and coupling differ, however, from those obtained by BCS theory due to the different structure of the number equation. It can be verified [15] from Eqs. (2)–(6) that the Bogoliubov approximation for the composite bosons is recovered in the strong-coupling ($\beta\mu \to -\infty$ and $\Delta \ll |\mu|$) limit. This represents a notable achievement of our theory.

The use of bare BCS single-particle Green's functions in the self-energy (1) further enables us to perform the analytic continuation to real frequency ω in a closed form, as to avoid numerical extrapolation procedures. To this end, and similarly to what was done in Ref. [14] for the normal phase, we express the pairing-fluctuation propagator Γ_{11} by its spectral representation:

$$\Gamma_{11}(\mathbf{q}, \Omega_\nu) = -\frac{1}{\pi} \int_{-\infty}^{+\infty} d\omega' \frac{\mathrm{Im}\Gamma_{11}(\mathbf{q}, \omega')}{i\Omega_\nu - \omega'}. \quad (8)$$

Here $\mathrm{Im}\Gamma_{11}(\mathbf{q},\omega)$ is defined as the imaginary part of $\Gamma_{11}(\mathbf{q}, i\Omega_\nu \to \omega + i\eta)$. This quantity is, in turn, obtained from the expressions (2)–(4), with the replacement $i\Omega_\nu \to \omega + i\eta$ made *after* the sum over the internal (Matsubara) frequency has been performed. In this way, the imaginary part of the retarded self-energy Σ_{11}^R is

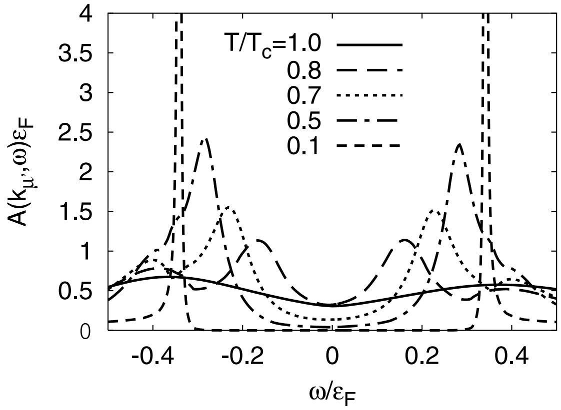

FIG. 1. Single-particle spectral function vs frequency (in units of ε_F) at different temperatures, for $|\mathbf{k}| = k_{\mu'}$ and $(k_F a_F)^{-1} = -0.45$. (See Ref. [16] for the definition of $k_{\mu'}$.)

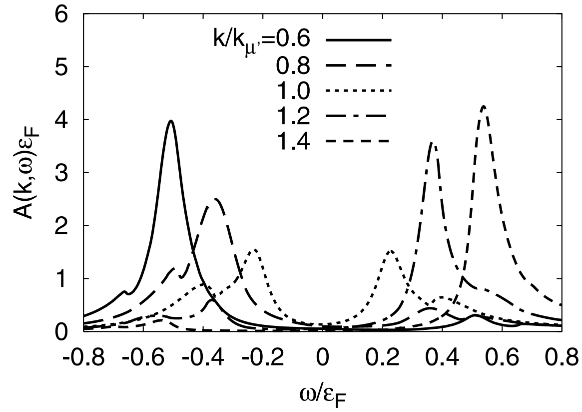

FIG. 2. Single-particle spectral function vs frequency (in units of ε_F) at different wave vectors about $k_{\mu'}$, for $T = 0.7T_c$ and $(k_F a_F)^{-1} = -0.45$.

$$\mathrm{Im}\Sigma_{11}^R(\mathbf{k},\omega) = -\int \frac{d\mathbf{q}}{(2\pi)^3}\big(u_{\mathbf{q}-\mathbf{k}}^2 \mathrm{Im}\Gamma_{11}[\mathbf{q},\omega + E(\mathbf{q}-\mathbf{k})] \times \{f[E(\mathbf{q}-\mathbf{k})] + b[\omega + E(\mathbf{q}-\mathbf{k})]\} + v_{\mathbf{q}-\mathbf{k}}^2 \mathrm{Im}\Gamma_{11}[\mathbf{q},\omega - E(\mathbf{q}-\mathbf{k})] \times \{f[-E(\mathbf{q}-\mathbf{k})] + b[\omega - E(\mathbf{q}-\mathbf{k})]\}\big). \tag{9}$$

Here $f(x) = [\exp(\beta x) + 1]^{-1}$ and $b(x) = [\exp(\beta x) - 1]^{-1}$ are the Fermi and Bose distributions, while $u_{\mathbf{k}}^2$ and $v_{\mathbf{k}}^2$ are the usual BCS coherence factors. The real part of Σ_{11}^R is then obtained via a Kramers-Kronig transform. The retarded single-particle Green's function G_{11}^R results from these functions, in terms of which single-particle spectral function $A(\mathbf{k},\omega) = -\frac{1}{\pi}\mathrm{Im}G_{11}^R(\mathbf{k},\omega)$ of interest is eventually obtained as a function of ω for any given $\mathbf{k}$ [16].

Figure 1 shows the evolution with temperature of the single-particle spectral function for an intermediate coupling $[(k_F a_F)^{-1} = -0.45]$. [For this coupling, the ratio of the pair-breaking temperature T^* to the critical temperature T_c is about 1.25, as obtained in Ref. [14].] Focusing specifically on the features at negative ω, note how the (sharp) coherent peak grows from the (broad) pseudogap structure already present at T_c. The coherent peak becomes sharper upon lowering the temperature and gains weight at the expense of the pseudogap structure, giving rise to a characteristic peak-dip-hump profile. The two features coexist over a wide range of temperature.

Figure 2 shows the wave-vector dependence of the single-particle spectral function at the temperature $T = 0.7T_c$ for the same coupling in Fig. 1. Following the evolution of the coherent peak across the underlying Fermi surface, one identifies the characteristic particle-hole mixing of the BCS theory, with a reflection of both particle and hole bands accompanied by a transfer of the spectral weight from negative to positive frequencies. In our theory, such BCS-like features coexist with non-BCS behaviors, namely, the occurrence of the pseudogap structure and the strong temperature dependence of the spectral weight of the coherent peak (see Fig. 4 below).

Figures 3(a) and 3(b) report, respectively, the weight z and position Δ_{m} of the coherent peak of the single-particle spectral function at negative frequencies vs coupling for a low temperature ($T = 0.1T_c$). The weight z of the coherent peak was determined by fitting the peak with a Lorentzian distribution. This fitting was performed by considering only the right half of the peak. The tail of the peak toward positive frequencies was further truncated at zero frequency. In this way, we

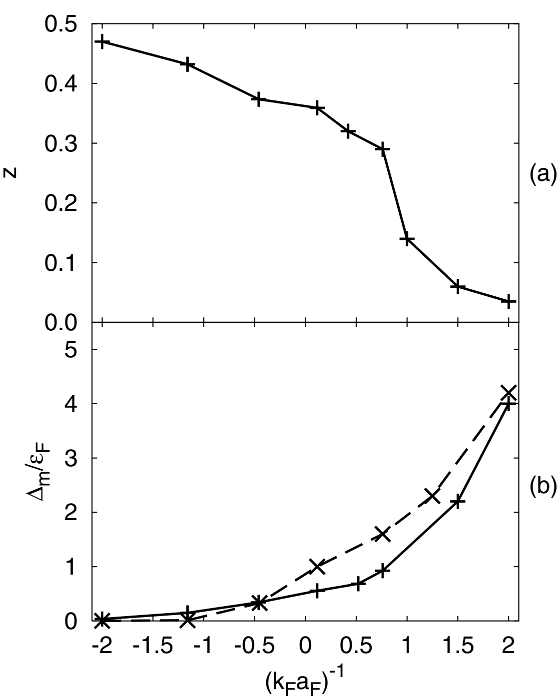

FIG. 3. (a) Weight z and (b) position Δ_{m} (solid line) of the coherent peak at negative frequencies vs coupling for $T = 0.1T_c$. In (b) the pseudogap Δ_{pg} for $T = T_c$ (dashed line) is also shown.

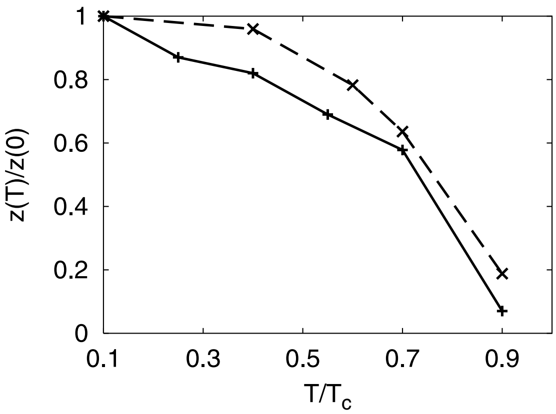

FIG. 4. Temperature dependence of the weight z of the coherent peak at negative frequencies (solid line) for $(k_F a_F)^{-1} = -0.45$. The superfluid density ρ_s (dashed line) is also shown for comparison.

managed to reduce the background signal due to the broad pseudogap structure, on the one hand, and to the peak feature at positive frequencies, on the other hand. The peak weight z saturates at the BCS value 0.5 in weak coupling, decreases markedly across the crossover region $-1 \lesssim (k_F a_F)^{-1} \lesssim +1$, and becomes negligible in strong coupling. At the same time, the peak position Δ_m increases monotonically across the crossover region. In Fig. 3(b) we also report the pseudogap Δ_{pg} (dashed line), as identified from the position of the maximum of the spectral function at T_c. While the qualitative trend of Δ_m and Δ_{pg} vs coupling is similar, the two curves cross each other at about the intermediate-coupling value $(k_F a_F)^{-1} = -0.45$. In addition, we have verified that Δ_m nearly coincides with the value of the order parameter Δ in the weak-to-intermediate coupling region.

Figure 4 reports the dependence of the weight z on temperature for the coupling value $(k_F a_F)^{-1} = -0.45$ (solid line). Note the strong temperature dependence of this quantity, which vanishes at T_c. This contrasts the BCS behavior, whereby the weight of the coherent peak for negative frequencies would equal 0.5 irrespective of temperature. The temperature dependence of the superfluid density ρ_s (calculated according to Ref. [17]) is also shown in the figure (dashed line). The resemblance between these two quantities has been noted experimentally for nearly optimally doped cuprates [9,10]. We have, however, verified that this resemblance does not occur for other values of the coupling, both on the weak- and strong-coupling sides of the crossover. On the weak-coupling side of the crossover, in particular, our finding is confirmed by the BCS theory, whereby $z = 0.5$ irrespective of temperature while ρ_s decreases monotonically from $T = 0$ to T_c. For this reason, no universal correspondence between the temperature dependence of z and ρ_s should be expected on physical grounds.

In conclusion, we have shown that pairing fluctuations can (at least qualitatively) account for several nontrivial features of single-particle spectra in the superconducting state. Our results specifically demonstrate that the experimental finding of two distinct features (pseudogap structure and coherent peak) in the single-particle spectral function is fully consistent with the occurrence of strong pairing fluctuations in cuprate superconductors. Competition of two distinct order parameters is therefore not required to account for the occurrence of two different energy scales in the experimental data.

We are indebted to A. Perali for discussions. Financial support from the Italian MIUR under Contract No. COFIN 2001 Prot. 2001023848 is gratefully acknowledged.

[1] A. Damascelli, Z-X. Shen, and Z. Hussain, Rev. Mod. Phys. **75**, 473 (2003), and references therein.
[2] M. Kugler *et al.*, Phys. Rev. Lett. **86**, 4911 (2001).
[3] D. L. Feng *et al.*, Phys. Rev. Lett. **86**, 5550 (2001); Y.-D. Chuang *et al.*, *ibid.* **87**, 117002 (2001); A. A. Kordyuk *et al.*, *ibid.* **89**, 077003 (2002).
[4] A. D. Gromko *et al.*, cond-mat/0205385.
[5] Y. Wang *et al.*, Science **299**, 86 (2003).
[6] M. Eschrig and M. R. Norman, Phys. Rev. Lett. **89**, 277005 (2002); G. Seibold and M. Grilli, Phys. Rev. B **63**, 224505 (2001).
[7] J. C. Campuzano *et al.*, Phys. Rev. B **53**, R14 737 (1996).
[8] H. Matsui *et al.*, Phys. Rev. Lett. **90**, 217002 (2003).
[9] D. L. Feng *et al.*, Science **280**, 277 (2000).
[10] H. Ding *et al.*, Phys. Rev. Lett. **87**, 227001 (2001).
[11] V. M. Krasnov, Phys. Rev. B **65**, 140504(R) (2002).
[12] V. N. Zavaritsky, cond-mat/0306081.
[13] P. Nozières and S. Schmitt-Rink, J. Low Temp. Phys. **59**, 195 (1985).
[14] A. Perali, P. Pieri, G. C. Strinati, and C. Castellani, Phys. Rev. B **66**, 024510 (2002).
[15] P. Pieri, L. Pisani, and G.C. Strinati (unpublished).
[16] As was done in Ref. [14] above T_c, in the weak-to-intermediate coupling region we found it necessary to introduce the constant shift $\Sigma_0 = \mathrm{Re}\Sigma_{11}^R(|\mathbf{k}| = k_{\mu'}, \omega = 0)$ in the BCS single-particle Green's functions entering Eqs. (1)–(4). This shift plays in the present context an analogous role to the Hartree shift for the negative-U Hubbard model. With this shift, $A(\mathbf{k}, \omega)$ has a local minimum for $\omega = 0$ at the Fermi surface crossing, where $|\mathbf{k}|$ takes the value $k_{\mu'} = \sqrt{2m\mu'}$ for $\mu' > 0$ with $\mu' = \mu - \Sigma_0$. The spectra for $A(\mathbf{k}, \omega)$ are shown in the text for this special values of $|\mathbf{k}|$.
[17] N. Andrenacci, P. Pieri, and G. C. Strinati, Phys. Rev. B **68**, 144507 (2003).